Stochastic phase space dynamics with constraints for molecular systems

W. Paul* and D. Y. Yoon
IBM Research Division, Almaden Research Center, 650 Harry Road, San Jose, California 95120-6099
(Received 30 March 1994; revised manuscript received 29 December 1994)

Constraining fast degrees of freedom and using a Langevin-like description of the dynamics are standard tools to simulate complex systems that allow for comparatively large time steps in the numerical integration of the equations of motion. Here we start with the Hamiltonian description of classical mechanics for the incorporation of stochastic and frictional forces. Constraints are incorporated into Hamiltonian dynamics following a procedure put forward by Dirac. Combining these two approaches, in general, requires a different treatment of the constraints from that which is usually done in deterministic dynamics. The numerical algorithm we chose for the integration of these equations is a second-order Runge-Kutta scheme modified by a Euler treatment for the constraints. The resulting algorithm is stable up to large time steps and generates averages in the canonical ensemble. The applicability of the method to the simulation of large molecular systems is shown for a melt of n-C_{13} alkane chains by a comparison to results from a Nosé-Hoover molecular dynamics simulation.

PACS number(s): 02.70.Ns, 36.20.−r, 61.25.Hq

I. INTRODUCTION

Computer simulation of dense systems of complex molecules (e.g., polymers) is an example of a computational task easily probing the limits of existing computational capabilities. Treating the degrees of freedom from the scale of the bond length to the size of the entire molecule and obtaining the configurational equilibration of the melt usually requires dealing with more than six decades in relaxation times. A constant energy molecular dynamics (MD) simulation that uses a time step of $10^{-3}-10^{-2}$ times the smallest relaxation time would have to run numerically stable for at least 10^8 integration steps. While this may be computationally feasible using a stable integration scheme such as the Verlet algorithm, the resulting algorithm would be prohibitively slow. Besides changing the model completely (using lattice models and/or Monte Carlo techniques, for example) there are two approaches to overcoming this problem: constraining the fastest degrees of freedom and changing the simulated ensemble to a canonic one. The latter can be achieved by using the extended system of the Nosé-Hoover [1,2] approach or by going from a MD simulation to a stochastic dynamics (SD) simulation that augments the deterministic equations of motion with stochastic and frictional forces [3,4].

The main purpose in both schemes is to change the simulated thermodynamic ensemble, but since they introduce an effective restoring force that keeps the temperature to a mean value, they also lead to an increased stability of the numerical integration algorithms as compared to a constant energy MD method [5,6]. Constraining the fastest degrees of freedom in our example means fixing the bond lengths. The method for incorporating such constraints into standard and extended system MD simulations on the basis of the Lagrangian approach to Newtonian dynamics as well as the algorithms for their numerical implementation have been extensively reviewed [7,8].

The use of stochastic dynamics for the simulation of alkane chain systems has been discussed in Ref. [4] in a configuration space approach. The derivation of that algorithm did not explicitly consider constraints that were treated as in the standard Lagrangian case. We will show later on that this need not necessarily be so. In this paper, we present a phase space description of the dynamics that correctly incorporates the constraints along with standard treatments of stochastic differential equations. Section II will present an exposition of Hamiltonian dynamics with constraints following Dirac's ideas [9] since this topic is rarely treated and we will need the results for further reference. In Sec. III, we will show the extension of this Hamiltonian dynamics into a stochastic dynamics. The numerical algorithm for the integration of the thus derived equations of motion will be discussed in Sec. IV with respect to general results on numerical integrators for stochastic differential equations [10–12]. The results of the application of this algorithm to the simulation of melts of short alkane chains and a comparison to existing data in the literature [13] will be discussed in Sec. V, Sec. VI will present some conclusions, and an Appendix will give a few important technical details on the simulation.

II. HAMILTONIAN DYNAMICS WITH CONSTRAINTS

Curiously enough this problem seems to have been studied for the first time as late as 1950 by Dirac [9] and Anderson and Bergmann [14] as a starting point for incorporating constraints into quantum mechanics and quantum field theory. Recently, this problem has been discussed again by de Leeuw, Perram, and Petersen [15] with special emphasis on its relevance to the phase space

*Permanent address: Institut für Physik, Johannes Gutenberg Universität, D-55099 Mainz, Germany.

integrals occurring in statistical mechanics. There are basically two (equivalent) ways of going from a given Lagrangian and a set of holonomic constraints to a Hamiltonian description with constraints. They are discussed in detail and in a more mathematical terminology in [16] under the headings "vaconomic mechanics" (mechanics of the variational axiomatic kind) and "Hamiltonian dynamics with constraints." The basic idea is [16] that one either considers a constrained Lagrangian and uses this to define the conjugate momenta and the transition to the constrained Hamiltonian as was done in [15], or starts from the Hamiltonian description on the unconstrained manifold, adds the constraints to define a modified Hamiltonian, and generates the constrained Hamiltonian dynamics by the Poisson bracket with the modified Hamiltonian. This approach was taken by Dirac [9] and is more convenient for our purpose of introducing frictional forces for the stochastic dynamics since the conjugate momenta in this approach depend only on the velocities and not on the constraints. Let us, therefore, consider a dynamical system with Hamiltonian given by

$$\mathcal{H}(\{\vec{q}\},\{\vec{p}\})=\sum_i \frac{1}{2m_i}\vec{p}_i^{\,2}+V(\{\vec{q}\}) \ . \tag{1}$$

We furthermore consider the holonomic constraints

$$\Phi_k(\{\vec{q}\})=0, \quad k=1,\ldots,M \ , \tag{2}$$

and their differential form (or first time derivative)

$$\Psi_k(\{\vec{q}\},\{\vec{p}\})=\sum_i \frac{\partial\Phi_k}{\partial\vec{q}_i}\cdot\frac{\vec{p}_i}{m_i}=0 \ , \tag{3}$$

where we expressed the Cartesian velocities through their conjugate momenta. For treating mechanics with constraints, Eqs. (2) and (3) are equivalent. For the derivation of Hamiltonian dynamics with constraints, one uses (2) as the so-called primary constraints [16]. We will incorporate both (2) and (3) into our constrained Hamiltonian, which will show up as redundant information in the Hamiltonian case, but is helpful for the extension to a stochastic dynamics algorithm. So let us define the constrained Hamiltonian by

$$\mathcal{H}'(\{\vec{q}\},\{\vec{p}\})=\mathcal{H}(\{\vec{q}\},\{\vec{p}\})+\sum_{k=1}^{M}\lambda_k\Phi_k(\{\vec{q}\}) + \sum_{k=1}^{M}\mu_k\Psi_k(\{\vec{q}\},\{\vec{p}\}) \ . \tag{4}$$

The equations of motion resulting from this Hamiltonian are

$$\dot{\vec{q}}_i=\{\vec{q}_i,\mathcal{H}'\}=\frac{\vec{p}_i}{m_i}+\sum_{k=1}^{M}\mu_k\frac{\partial\Psi_k}{\partial\vec{p}_i} \ , \tag{5}$$

$$\dot{\vec{p}}_i=\{\vec{p}_i,\mathcal{H}'\}=\vec{F}_i-\sum_{k=1}^{M}\lambda_k\frac{\partial\Phi_k}{\partial\vec{q}_i}-\sum_{k=1}^{M}\mu_k\frac{\partial\Psi_k}{\partial\vec{q}_i} \ , \tag{6}$$

where $\{\ \}$ denotes the Poisson bracket. As additional requirements we have the time invariance of the constraint equations for motions on the constraint manifold,

$$\{\Phi_l,\mathcal{H}'\}=\sum_i\frac{\partial\Phi_l}{\partial\vec{q}_i}\cdot\frac{\vec{p}_i}{m_i}+\sum_{k=1}^{M}\mu_k\sum_i\frac{\partial\Phi_l}{\partial\vec{q}_i}\cdot\frac{\partial\Psi_k}{\partial\vec{p}_i}=0 \ , \tag{7}$$

$$\{\Psi_l,\mathcal{H}'\}=\sum_i\left[\frac{\partial\Psi_l}{\partial\vec{q}_i}\cdot\frac{\vec{p}_i}{m_i}+\frac{\partial\Psi_l}{\partial\vec{p}_i}\cdot\vec{F}_i\right] -\sum_{k=1}^{M}\lambda_k\sum_i\frac{\partial\Psi_l}{\partial\vec{p}_i}\cdot\frac{\partial\Phi_k}{\partial\vec{q}_i} +\sum_{k=1}^{M}\mu_k\sum_i\left[\frac{\partial\Psi_l}{\partial\vec{q}_i}\cdot\frac{\partial\Psi_k}{\partial\vec{p}_i}-\frac{\partial\Psi_l}{\partial\vec{p}_i}\cdot\frac{\partial\Psi_k}{\partial\vec{q}_i}\right]=0 \ . \tag{8}$$

Making use of the fact that

$$\Psi_k(\{\vec{q}\},\{\vec{p}\})=\sum_i\frac{\partial\Phi_k}{\partial\vec{q}_i}\cdot\frac{\vec{p}_i}{m_i} \ , \tag{9}$$

Eq. (7) reads

$$\sum_{k=1}^{M}\mu_k\sum_i\frac{1}{m_i}\frac{\partial\Phi_l}{\partial\vec{q}_i}\cdot\frac{\partial\Phi_k}{\partial\vec{q}_i}=0 \ . \tag{10}$$

The symmetric matrix

$$A_{lk}=\sum_i\frac{1}{m_i}\frac{\partial\Phi_l}{\partial\vec{q}_i}\cdot\frac{\partial\Phi_k}{\partial\vec{q}_i} \tag{11}$$

is, in general, nonsingular, so that Eq. (10) leads to

$$\mu_k=0, \quad k=1,\ldots,M \ . \tag{12}$$

Trying to use both constraint equations (2) and (3), we find that in the case of pure Hamiltonian dynamics, one of them is redundant. Using Eq. (2) as the primary constraints, Eq. (7) leads to the differential form of the constraint equation (3) as a secondary constraint [$\mu_k=0$ in (7)] and the time invariance of the secondary constraints gives a set of equations [(8) with all $\mu_k=0$] for the Lagrange parameters λ_k. The equations of motion and the determining equations for the Lagrange parameters are the same or equivalent to those in the Lagrangian treatment of constraint dynamics.

Before discussing the extension of this Hamiltonian dynamics to a stochastic dynamics, let us become more specific now and write down the equations of motion for a united atom model of a melt of linear alkane chains CH_3-$(CH_2)_{N-2}$-CH_3. We will keep the C-C bond length fixed and treat the CH_2 and CH_3 groups as united atoms of mass 14 a.u. and 15 a.u., respectively. The exact force fields will be specified in Sec. V. The constraint equations take the form

$$\Phi_k^\alpha(\{\vec{q}\})=(\vec{q}_{k+1}^{\,\alpha}-\vec{q}_k^{\,\alpha})^2-l^2=0 \ , \quad k=1,\ldots,N-1;\alpha=1,\ldots,P \tag{13}$$

$$\Psi_k^\alpha(\{\vec{q}\},\{\vec{p}\})=(\vec{q}_{k+1}^{\,\alpha}-\vec{q}_k^{\,\alpha})\cdot\left[\frac{\vec{p}_{k+1}^{\,\alpha}}{m_{k+1}}-\frac{\vec{p}_k^{\,\alpha}}{m_k}\right]=0 \ , \quad k=1,\ldots,N-1; \ \alpha=1,\ldots,P \ , \tag{14}$$

where N is the number of united atoms per chain, l is the

C-C bond length, and P is the number of chains in the simulation volume. The equations of motion have the following form:

$$\dot{\vec{q}}_i^{\alpha}=\frac{\vec{p}_i^{\alpha}}{m_i}+\frac{\mu_{i-1}^{\alpha}}{m_i}(\vec{q}_i^{\alpha}-\vec{q}_{i-1}^{\alpha})-\frac{\mu_i^{\alpha}}{m_{i+1}}(\vec{q}_{i+1}^{\alpha}-\vec{q}_i^{\alpha}) , \tag{15}$$

$$\dot{\vec{p}}_i^{\alpha}=\vec{F}_i^{\alpha}-\mu_{i-1}^{\alpha}\left[\frac{\vec{p}_i^{\alpha}}{m_i}-\frac{\vec{p}_{i-1}^{\alpha}}{m_{i-1}}\right]+\mu_i^{\alpha}\left[\frac{\vec{p}_{i+1}^{\alpha}}{m_{i+1}}-\frac{\vec{p}_i^{\alpha}}{m_i}\right]$$
$$-2\lambda_{i-1}^{\alpha}(\vec{q}_i^{\alpha}-\vec{q}_{i-1}^{\alpha})+2\lambda_i^{\alpha}(\vec{q}_{i+1}^{\alpha}-\vec{q}_i^{\alpha}) . \tag{16}$$

We will not write down the explicit version of the consistency equations (7) and (8) following from the time invariance of the constraints, since we will not use them for the algorithm.

III. STOCHASTIC PHASE SPACE DYNAMICS WITH CONSTRAINTS

To extend the Hamiltonian dynamics with constraints into a stochastic dynamics in phase space we augment Eqs. (15) and (16) [in the general formulation Eqs. (5) and (6)] by stochastic and frictional forces. Since frictional forces are proportional to the momenta, using the velocities $\vec{v}_i=\vec{p}_i/m_i$ as the second phase space variable, one gets

$$d\vec{q}_i^{\alpha}=\vec{v}_i^{\alpha}dt+\left[\frac{\mu_{i-1}^{\alpha}}{m_i}(\vec{q}_i^{\alpha}-\vec{q}_{i-1}^{\alpha})-\frac{\mu_i^{\alpha}}{m_{i+1}}(\vec{q}_{i+1}^{\alpha}-\vec{q}_i^{\alpha})\right]dt , \tag{17}$$

$$m_i d\vec{v}_i^{\alpha}=[\vec{F}_i^{\alpha}-\gamma m_i\vec{v}_i^{\alpha}]dt+[\mu_i^{\alpha}(\vec{v}_{i+1}^{\alpha}-\vec{v}_i^{\alpha})-\mu_{i-1}^{\alpha}(\vec{v}_i^{\alpha}-\vec{v}_{i-1}^{\alpha})]dt$$
$$+[2\lambda_i^{\alpha}(\vec{q}_{i+1}^{\alpha}-\vec{q}_i^{\alpha})-2\lambda_{i-1}^{\alpha}(\vec{q}_i^{\alpha}-\vec{q}_{i-1}^{\alpha})]dt$$
$$+\sigma_i d\vec{W}_i^{\alpha}(t) , \tag{18}$$

where γ is the friction coefficient and the $dW_{i\alpha}(t)$ are the increments of independent Wiener processes,

$$\langle dW_{i\alpha}(t)\rangle=0 ,$$
$$\langle dW_{i\alpha}(t)dW_{j\beta}(t')\rangle=\delta_{ij}\delta_{\alpha\beta}\delta(t-t')dt . \tag{19}$$

The prefactor σ_i is fixed by the fluctuation dissipation theorem

$$\sigma_i^2=2\gamma m_i k_B T . \tag{20}$$

Note that now we cannot conclude that either all λ_i^{α} or all μ_i^{α} are equal to zero since the dynamics imposed by Eqs. (17) and (18) is no longer Hamiltonian. The consistency equations (7) and (8) are no longer directly available to determine the Lagrange parameters λ_i^{α} and μ_i^{α}. This was overlooked in Ref. [4] where the corresponding equations for the Lagrangian dynamics were still used to derive the numerical algorithm for the integration of the equations of motion, though not actually used to calculate the values of the Lagrange parameters.

The general idea when calculating the forces of constraint is the same as in the deterministic case. The constraint equations have to be invariant under the dynamics generated by the equations of motion. To implement this idea for the stochastic dynamics, we have to remember that the solutions to the equations of motion (17) and (18) are defined as the solutions to the following stochastic integral equations:

$$\vec{q}_i^{\alpha}(t)-\vec{q}_i^{\alpha}(0)=\int_0^t\vec{v}_i^{\alpha}(t')dt'$$
$$+\int_0^t\left\{\frac{\mu_{i-1}^{\alpha}(t')}{m_i}[\vec{q}_i^{\alpha}(t')-\vec{q}_{i-1}^{\alpha}(t')]-\frac{\mu_i^{\alpha}(t')}{m_{i+1}}[\vec{q}_{i+1}^{\alpha}(t')-\vec{q}_i^{\alpha}(t')]\right\}dt' \tag{21}$$

and

$$m_i[\vec{v}_i^{\alpha}(t)-\vec{v}_i^{\alpha}(0)]=\int_0^t[\vec{F}_i^{\alpha}(t')-\gamma m_i\vec{v}_i^{\alpha}(t')]dt'+\sigma_i\int_0^t d\vec{W}_i^{\alpha}(t')$$
$$+\int_0^t\{\mu_i^{\alpha}(t')[\vec{v}_{i+1}^{\alpha}(t')-\vec{v}_i^{\alpha}(t')]-\mu_{i-1}^{\alpha}(t')[\vec{v}_i^{\alpha}(t')-\vec{v}_{i-1}^{\alpha}(t')]\}dt'$$
$$+\int_0^t\{2\lambda_i^{\alpha}(t')[\vec{q}_{i+1}^{\alpha}(t')-\vec{q}_i^{\alpha}(t')]-2\lambda_{i-1}^{\alpha}(t')[\vec{q}_i^{\alpha}(t')-\vec{q}_{i-1}^{\alpha}(t')]\}dt' . \tag{22}$$

Inserting these equations into the constraint equations (2) and (3) gives the defining equations for the determination of the Lagrange parameters in the case of the stochastic dynamics. They are nonlinear stochastic integral equations and of not much practical use in this general form. However, when combined with the chosen algorithm for the integration of the stochastic equations of motion, which amounts to a certain order up to which the integral equations above are solved, this definition yields a procedure to determine the Lagrange parameters to the same order as the integration algorithm.

Alternatively, one can look at the total stochastic differential of the constraint equations (2) and (3) making use of the equations of motion (17) and (18). Here we need only to consider the differences appearing in comparison to the Hamiltonian case. The important one is the term

$$(\vec{q}_{i+1}^{\alpha}-\vec{q}_i^{\alpha})\cdot\left[\frac{\sigma_{i+1}}{m_{i+1}}d\vec{W}_{i+1}^{\alpha}-\frac{\sigma_i}{m_i}d\vec{W}_i^{\alpha}\right] \tag{23}$$

appearing in the differential of Eq. (3). If the stochastic

velocity increments are chosen orthogonal to the constraints so that the above term is zero, one is back to the case of the consistency equations in the Hamiltonian dynamics. The two constraints are redundant and only one set of Lagrange parameters needs to be considered. In the numerical implementation, this set would be used to guarantee the fulfillment of Eq. (2), but one would have to correct the velocities from time to time because of the violation of (3) due to numerical inaccuracies (if one does an integration in phase space). Furthermore, since we are using Cartesian and not generalized coordinates, the Wiener increments $d\vec{W}_i^{\alpha}$ would no longer be independent along the chain and one would have to reexamine the fluctuation dissipation relation.

However, if one envisages the stochastic forces as modeling uncontrolled fast degrees of freedom, one would not, in general, require the term (23) to vanish. In this case, the two sets of Lagrange parameters are no longer redundant. In the numerical implementation, they will be used to fulfill both constraint equations separately. Also, now the Wiener increments are independent variables and the choice of the σ_i according to the fluctuation-dissipation relation (20) leads to the correct mean kinetic energy of the center of mass of a chain.

In the next section, we will discuss how one integrates the stochastic differential equations taking into account the constraints in this way and we will present the algorithm we chose.

IV. NUMERICAL INTEGRATION OF STOCHASTIC PHASE SPACE DYNAMICS WITH CONSTRAINTS

As a reminder of the general results on the numerical integration of stochastic differential equations and for later reference, let us briefly discuss the following general equations:

$$dz_i = f_i(z,t)dt + \sigma dW_i \ , \tag{24}$$

with $z_i, f_i, dW_i \in R^n$. The simplest integration scheme is the Euler algorithm with time step h

$$z_i(h) = z_i(0) + f_i(z(0),0)h + \sigma \Delta W_i(h) + O(h^2) \ , \tag{25}$$

where $\Delta W_i(h)$ is a Gaussian random variable with zero mean and variance h. The Euler algorithm is first order in h and every moment of the random variables z_i at a fixed time t will be known up to an error $O(h)$. The highest-order algorithms for these stochastic differential equations are of second order in a single integration step [10,11] leading to errors $O(h^2)$ for the moments of the stochastic variables at fixed time t. The simplest integration scheme having this order of accuracy is the Heun algorithm [12,17], which is a second-order Runge-Kutta scheme [18],

$$z_i(h) = z_i(0) + \tfrac{1}{2}h\,[f_i(z(0),0) + f_i(\xi(h),h)] + \sigma \Delta W_i(h) + O(h^3) \tag{26}$$

involving one Euler step for the determination of the $\xi_i(h)$,

$$\xi_i(h) = z_i(0) + f_i(z(0),0)h + \sigma \Delta W_i(h) \ . \tag{27}$$

Turning to our equations of motion (17) and (18), let us denote the Euler step for the positions by $\vec{\xi}_i^{\alpha}(h)$ and the one for the velocities by $\vec{\omega}_i^{\alpha}(h)$. They are

$$\vec{\xi}_i^{\alpha}(h) = \vec{q}_i^{\alpha}(0) + \vec{v}_i^{\alpha}(0)h + \left\{ \frac{\mu_{i-1}^{\alpha}(0)}{m_i}[\vec{q}_i^{\alpha}(0) - \vec{q}_{i-1}^{\alpha}(0)] - \frac{\mu_i^{\alpha}(0)}{m_{i+1}}[\vec{q}_{i+1}^{\alpha}(0) - \vec{q}_i^{\alpha}(0)] \right\} h \ , \tag{28}$$

$$m_i \vec{\omega}_i^{\alpha}(h) = m_i \vec{v}_i^{\alpha}(0) + [\vec{F}_i^{\alpha}(0) - \gamma m_i \vec{v}_i^{\alpha}(0)]h + \sigma_i \Delta \vec{W}_i^{\alpha}(h) + \{\mu_i^{\alpha}(0)[\vec{v}_{i+1}^{\alpha}(0) - \vec{v}_i^{\alpha}(0)] - \mu_{i-1}^{\alpha}(0)[\vec{v}_i^{\alpha}(0) - \vec{v}_{i-1}^{\alpha}(0)]\}h + \{2\lambda_i^{\alpha}(0)[\vec{q}_{i+1}^{\alpha}(0) - \vec{q}_i^{\alpha}(0)] - 2\lambda_{i-1}^{\alpha}(0)[\vec{q}_i^{\alpha}(0) - \vec{q}_{i-1}^{\alpha}(0)]\}h \ . \tag{29}$$

Inserting these predictions into the constraint equations, one would get the determining equations for the Lagrange parameters corresponding to the Euler scheme. These will be solved using the SHAKE computer algorithm [7,8] for the determination of the constraint positions and velocities. But the limited accuracy of the Euler scheme in a practical implementation also enforces rather small time steps to insure fulfillment of the constraints.

Let us, therefore, now look at the Heun prediction for the positions,

$$\vec{q}_i^{\alpha}(h) = \vec{q}_i^{\alpha}(0) + \tfrac{1}{2}h\,[\vec{v}_i^{\alpha}(0) + \vec{\omega}_i^{\alpha}(h)] + \frac{1}{2}h \left\{ \frac{\mu_{i-1}^{\alpha}(0)}{m_i}[\vec{q}_i^{\alpha}(0) - \vec{q}_{i-1}^{\alpha}(0)] - \frac{\mu_i^{\alpha}(0)}{m_{i+1}}[\vec{q}_{i+1}^{\alpha}(0) - \vec{q}_i^{\alpha}(0)] \right\} + \frac{1}{2}h \left\{ \frac{\mu_{i-1}^{\alpha}(h)}{m_i}[\vec{\xi}_i^{\alpha}(h) - \vec{\xi}_{i-1}^{\alpha}(h)] - \frac{\mu_i^{\alpha}(h)}{m_{i+1}}[\vec{\xi}_{i+1}^{\alpha}(h) - \vec{\xi}_i^{\alpha}(h)] \right\} . \tag{30}$$

Without actually inserting the Euler predictions at this point, we state the following findings. Inserting the Euler prediction for the positions into the terms involving the constraints creates couplings to neighboring constraints along the chains that are quadratic in the time step and the Lagrange parameters. Furthermore, we have to determine $\mu_i^{\alpha}(h)$ for the forces of constraint corresponding to the Euler predictions at time h. Due to the nonlinearity of the constraint equations, this would involve solving coupled quadratic equations for the $\mu_i^{\alpha}(h)$.

In order to keep the integration scheme simple, we neglect at this point quadratic terms in the time step

when they involve the forces of constraint and substitute $\mu_i^\alpha(0)$ for $\mu_i^\alpha(h)$ and $\lambda_i^\alpha(0)$ for $\lambda_i^\alpha(h)$. This way we generate an algorithm that is of the order of the Heun scheme for all terms but the constraints and of the order of the Euler scheme for the constraints. That means the combined algorithm can only be shown to be correct to first order, although more exact and, from practical experience, more stable than the Euler scheme. Note, however, that the actual treatment of the constraints will be done with the SHAKE algorithm, which means that the positions and velocities after the integration step will differ from the correct ones by terms of the order this integration scheme has in all terms but the constraints. The reason for this is that the forces of constraint determined according to the integration scheme differ from the exact ones by terms of the order of the integration scheme, whereas the accuracy of the SHAKE determination is not connected to the order of the algorithm but to the desired numerical accuracy one chooses for the fulfillment of the constraints. As we will see in the application in the next section, this leads to a second-order algorithm in the end. The following are the equations for this numerical integrator:

$$\vec{q}_i^\alpha(h)=\vec{q}_i^\alpha(0)+\vec{v}_i^\alpha(0)h(1-\tfrac{1}{2}\gamma h)+\tfrac{1}{2}h^2\vec{F}_i^\alpha(0)+\tfrac{1}{2}\sigma_i h\Delta\vec{W}_i^\alpha(h)$$
$$+h\left\{\frac{\mu_{i-1}^\alpha(0)}{m_i}[\vec{q}_i^\alpha(0)-\vec{q}_{i-1}^\alpha(0)]-\frac{\mu_i^\alpha(0)}{m_{i+1}}[\vec{q}_{i+1}^\alpha(0)-\vec{q}_i^\alpha(0)]\right\}, \tag{31}$$

$$m_i\vec{v}_i^\alpha(h)=m_i\vec{v}_i^\alpha(0)+\tfrac{1}{2}h(1-\gamma h)\vec{F}_i^\alpha(0)+\tfrac{1}{2}h\vec{F}_i^\alpha(\{\vec{q}(h)\})-\gamma h(1-\tfrac{1}{2}\gamma h)m_i\vec{v}_i^\alpha(0)+\sigma_i(1-\tfrac{1}{2}\gamma h)\Delta\vec{W}_i^\alpha(h)$$
$$+h\{\mu_i^\alpha(0)[\vec{v}_{i+1}^\alpha(0)-\vec{v}_i^\alpha(0)]-\mu_{i-1}^\alpha(0)[\vec{v}_i^\alpha(0)-\vec{v}_{i-1}^\alpha(0)]\}$$
$$+h\{2\lambda_i^\alpha(0)[\vec{q}_{i+1}^\alpha(0)-\vec{q}_i^\alpha(0)]-2\lambda_{i-1}^\alpha(0)[\vec{q}_i^\alpha(0)-\vec{q}_{i-1}^\alpha(0)]\}\ . \tag{32}$$

Here we have incorporated the fact that we can replace $h\vec{F}_i^\alpha(\{\vec{\xi}(h)\})$ by $h\vec{F}_i^\alpha(\{\vec{q}(h)\})$ without changing the order of the treatment of the deterministic forces. These equations, together with the SHAKE scheme to determine the effect of the forces of constraint, define the numerical integration scheme.

Before we turn to the application, let us note that the SHAKE scheme fulfills the constraints by working through their effect on the positions and velocities of the atoms iteratively. Once the constraints are fulfilled to the desired accuracy, the differences

$$\delta\vec{q}_i^\alpha=\vec{q}_i^\alpha(h)-\tilde{\vec{q}}_i^\alpha(h)\ ,$$
$$\delta\vec{v}_i^\alpha=\vec{v}_i^\alpha(h)-\tilde{\vec{v}}_i^\alpha(h)\ , \tag{33}$$

the $\tilde{\vec{q}}_i^\alpha(h)$ and $\tilde{\vec{v}}_i^\alpha(h)$ being the predicted positions and velocities without taking into account the constraints, can be used to determine the Lagrange parameters μ_i^α and λ_i^α. However, they will only be known to the accuracy with which we treated the constraints in the numerical integration scheme, which is $O(h)$. A quantity like the pressure, which explicitly depends on the forces of constraint, will therefore contain a contribution that is only known to order $O(h)$.

V. SIMULATION OF A UNITED ATOM MODEL FOR *n*-TRIDECANE ($C_{13}H_{28}$) MELTS

In this section, we want to apply the algorithm defined in the preceding section to simulate a melt of 60 *n*-tridecane ($C_{13}H_{28}$) chains modeled as chains of united atoms of mass 14 a.u. and 15 a.u., respectively. A periodic cubic box of linear dimension 30.6 Å is used at 450 K and one of linear dimension 29.14 Å is used for 312 K to reproduce the experimental density at these two temperatures [19]. We will compare our findings on the static properties of these melts to results obtained by simulations of the same system using the Nosé-Hoover MD [1,13] method. The parameters used in the following are the same as those in [13]. The united atom force centers are located at the positions of the C atoms and the C-C bond length is kept fixed at 1.53 Å. The C-C-C bending motion is subject to the potential

$$U_b(\vartheta)=k_\vartheta[\cos(\vartheta)-\cos(\vartheta_0)]^2\ , \tag{34}$$

where $k_\vartheta=120$ kcal/mole and $\vartheta_0=1.95477$ rad and the torsional potential is given as

$$U_t(\phi)=\tfrac{1}{2}\{k_1[1-\cos(\phi)]+k_2[1-\cos(2\phi)]$$
$$+k_3[1-\cos(3\phi)]\}\ , \tag{35}$$

where $k_1=1.6$ kcal/mole, $k_2=-0.867$ kcal/mole, and $k_3=3.24$ kcal/mole. The nonbonded interaction is of the Lennard-Jones type

$$U_{\rm LJ}(r)=\begin{cases}\epsilon_0\left[\left[\dfrac{r_0}{r}\right]^{12}-2\left[\dfrac{r_0}{r}\right]^6\right], & r\le 2r_0\\ 0, & r>2r_0\ ,\end{cases} \tag{36}$$

where $r_0=4.5$ Å and $\epsilon_0=0.118$ kcal/mole. Most of the simulations have been performed at a temperature of 450 K where the conformational relaxation time of the chains is about 25 ps [13]. The value of the friction coefficient γ is set to the inverse of a Lennard-Jones-like time constant $\tau_0=(m_{\rm CH_2}l^2/\epsilon_0)^{1/2}=915.66$ fs. Runs of a total duration of 200-ps sampling about every 10 fs have been done at 450 K and nine different time steps ($h=1,1.5,2,2.5,3,4,6,8,10$ fs) have been used to assess the order of convergence of the algorithm. For the com-

TABLE I. Comparison of the results of the SPSD (stochastic phase space dynamics) algorithm with the Nosé-Hoover MD results, using the same time step of 1 fs, for n-tridecane melts at the experimental densities.

	SPSD	Nosé-Hoover MD	SPSD	Nosé-Hoover MD
T (K)	449.8	450	310.9	312
p (atm)	−250	−248	−230	−230
$C_N=\langle R^2\rangle/(N-1)l^2$	4.59	4.61	5.02	4.97
% *trans*	62	62	67	67
$D(10^{-6}$ cm^2/s)	31	46.4	6.3	7.0

parison with the Nosé-Hoover MD at 312 K, one run of 500 ps with a time sep of 1 fs has been performed sampling every 20 fs.

In Table I, we compare the pressure and conformational properties as obtained from the runs using the 1-fs time step to the Nosé-Hoover MD results obtained with the same time step. All the results are virtually identical, meaning that the P-V-T behavior and the conformational properties for this model are reproduced correctly by the new algorithm. The same holds true for the structural properties of the melt; for example, the pair distribution functions are found to be indistinguishable between the two simulation methods. Of course, a stochastic dynamics algorithm deviates in the dynamic behavior from that of a MD method due to the effect of the friction coefficient. This is evident when we look at the self-diffusion coefficient of the chains, which is also shown in Table I. The experimental value at 450 K is 50.9×10^{-6} cm^2/s and at 312 K it is 9.7×10^{-6} cm^2/s [20]. The values for the Nosé-Hoover MD method are quite close to the experiments for both temperatures whereas the values for the stochastic dynamics show larger deviations, especially at the higher temperature.

Now that this algorithm has been shown to generate the correct static properties at a small time step, we will examine the convergence behavior. Figure 1 shows the mean temperature as determined in the simulation as a function of the time step. Also shown is a fit with a quadratic time step dependence of the error with the prefactor of the quadratic behavior as the only fit parameter. The simulation results are nicely described by $T=450-0.4779h^2$, showing that the actual implementation of the algorithm using the SHAKE scheme to fulfill the constraints is of second order in a single time step and thus one order higher than what would be expected if the constraints were fulfilled according to the accuracy to which they are treated in the derivation of the algorithm. In support of this finding, Fig. 2 shows the mean bending energy and the mean torsional energy as linear functions of the square of the time step. The time step dependence of other quantities, like the mean squared radius of gyration and the mean squared end-to-end distance, are hard to assess due to the uncertainties in obtaining these values by these runs for 60 chains.

The error in the temperature for the largest time step of 10 fs in Fig. 1 is approximately 50 K. However, this is not due to a permanent drift in temperature, since, as shown in Fig. 3, the algorithm is still stable at this time step. That is, starting from an initial configuration corresponding to an internal temperature of 450 K the system temperature drops within the first few picoseconds to the average value typical for the chosen time step and then remains stable. The practical stability limit of this algorithm was found to be about 14 fs. At a time step of 15 fs, the integration becomes unstable within a few pi-

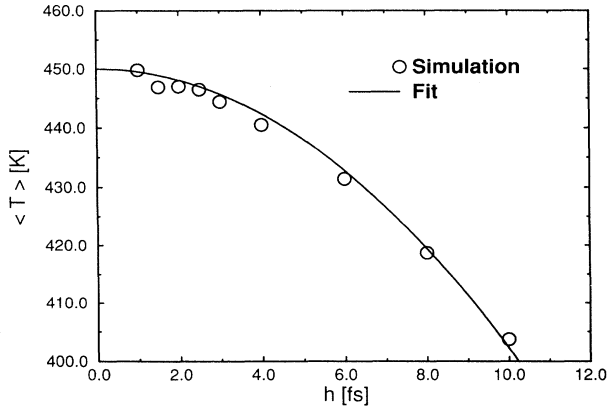

FIG. 1. The mean temperature as measured in the simulation as a function if the time step used (open circles). The full line is a one parameter fit to a quadratic time step dependence using the imposed temperature of 450 K as the zero time step limit.

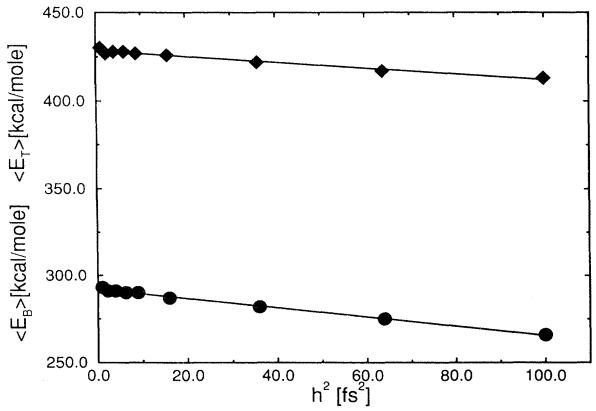

FIG. 2. Quadratic time step dependence of the mean bending energy E_b (full circles) and the mean torsional energy E_t (full diamonds). The straight lines are linear regressions to the data.

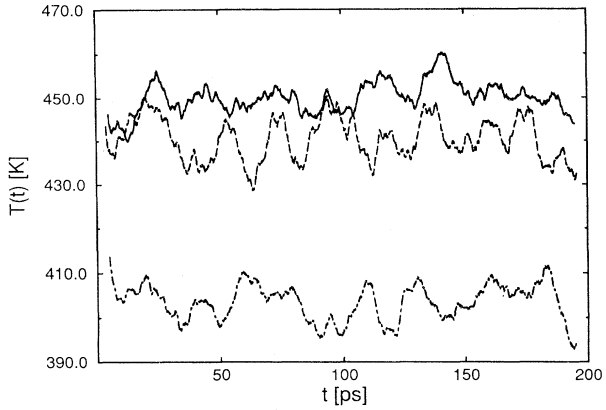

FIG. 3. Variation of the average temperature during the simulation as a function of time step, using an imposed temperature of 450 K. Full line, $h=1$ fs; dashed line, $h=4$ fs; and dot-dashed line, $h=10$ fs. The curves are running averages over 10 ps to reduce the fluctuations and emphasize the overall trend with the time step.

coseconds and the temperature diverges. One has to note that this is roughly one half of the time scale associated with the bond angle bending motions as the stiffest degrees of freedom, showing a rather high stability of this integration algorithm.

Now that we have shown that the algorithm is stable to very large time steps and also know by which amount the internal temperature is reduced when using the large time steps, we can of course try to correct that from the outset to equilibrate our system at the desired temperature by using the large time steps for the highest computational efficiency. Figure 4 shows the torsional angle distribution as determined for three runs where the target temperature has been adjusted to account for the expected temperature drop. The run with 1-fs time step was done with 450 K as the target temperature, the one with 4 fs used 460 K, and the one with 10 fs used 496 K. The three distributions are virtually identical even in the sensitive region of the barriers between the *trans* state and the *gauche* states. There is a slight reduction in the height of the *trans* maximum but when one looks at the average *trans* fraction, defined as the probability for ϕ to lie in between $-60°$ and 60°, this is practically independent of the time step (0.618 for $h=1$ fs, 0.617 for $h=4$ fs, and 0.614 for $h=10$ fs). Therefore, the drop in the height is compensated by a slight increase of the width of the *trans* peak meaning that the larger time steps allow for larger fluctuations around the mean *trans* position. The same is, of course, true for the *gauche* peaks but is not resolvable in the figure due to their smaller total weight. Overall, however, the conformational properties as well as the pressure and the pair distribution function come out the same for the three simulations. Static properties are only determined by the density and average temperature of the run, so that one can generate equilibrated structures at a certain temperature by using higher target temperatures for the large time steps.

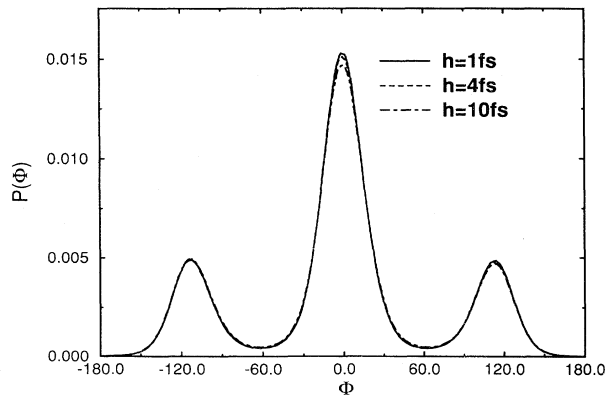

FIG. 4. Torsional angle distribution $P(\phi)$ for different time steps with target temperatures adjusted to yield mean temperatures of about 450 K in the simulation. Full line, $h=1$ fs; $\langle T\rangle=449.8$ K; dashed line, $h=4$ fs; $\langle T\rangle=450.4$ K; and dot-dashed line, $h=10$ fs; $\langle T\rangle=443.1$ K.

VI. CONCLUSIONS

We have shown in this paper that the extension to a stochastic dynamics is best done from a phase space or Hamiltonian description of the dynamics. The way to incorporate constraints into Hamiltonian dynamics has been reviewed and it has been shown that the extension into a stochastic dynamics, in general, requires a new treatment of the constraints differing from that which is derivable in either Lagrangian or Hamiltonian mechanics. The forces of constraint become stochastic variables and the integrated and differential forms of holonomic constraints, in general, are no longer redundant. In the derivation of the numerical algorithm to integrate the resulting equations of motion, the forces of constraint were only treated exactly to first order in the time step h, due to the numerically prohibitive complexity of the terms of order $h^{3/2}$ and h^2. Using the SHAKE algorithm for the exact fulfillment of the constraints along the generated trajectory, however, in practice also leads to a treatment of the constraints exact to order h^2 and, therefore, to an overall third-order algorithm for all quantities that do not explicitly depend on the forces of constraint. This was shown in the application to the simulation of *n*-tridecane melts. The advantage of this approach is that it leads to an algorithm that is stable up to very large time steps and that generates the correct averages of the canonical ensemble. The limiting stable time step is five times as large as the one for a Nosé-Hoover MD treatment of the same system as an alternative way to generate a *NVT* ensemble. The disadvantage is that the dynamics is changed by the introduction of the friction effects and depends on the chosen value of the friction coefficient. It is not changed qualitatively but the value of, for instance, the diffusion coefficient comes out wrong. Nevertheless, if one adjusts the temperature defining the strength of the stochastic forces to correct for the error in the simulation temperature induced by the large time steps, one has a very efficient method to equilibrate dense

systems of complex molecules with long intrinsic relaxation times.

ACKNOWLEDGMENTS

We are thankful to G. Smith for help with the simulation of alkane chain models and acknowledge helpful comments of D. Frenkel and J. P. Ryckaert. W.P. thanks IBM Germany for financial support.

APPENDIX

This Appendix will give a few technical details that are important to really use the algorithm derived in this paper efficiently. The most important point to note is that one does not need Gaussian random numbers for the numerical integration of a stochastic differential equation. This is of paramount importance in the simulation of a dense system. If one uses Gaussian random numbers, one not only invests a lot of CPU time unnecessarily (the usually employed Box-Muller algorithm to convert uniformly distributed random numbers into Gaussian distributed ones is far more CPU-time consuming than the random number generation itself) but one also has stochastic displacements in the positions and velocities that are not bounded. To reduce the probability of the occurrence of such a displacement in the length of the simulation, which could bring atoms too close together and cause a numeric overflow in the calculation of the nonbonded interaction, one has to resort to small time steps and the possible advantage of a stochastic dynamics simulation is lost. It was shown in [12] for the moments of the stochastic variables and in [21] and [22] for all properties of the stochastic process under study that it suffices to reproduce the first $2n$ moments of the Gaussian distribution if n is the order of the integration algorithm. The reported simulations used the following approximation for the Wiener process [12]:

$$\Delta W_{i\beta}(h)=\begin{cases}-(3h)^{1/2} & \text{if } R<1/6\\ 0 & \text{if } 1/6\le R<5/6\\ (3h)^{1/2} & \text{if } 5/6\le R\ ,\end{cases} \tag{A1}$$

where the random number R is uniformly distributed in (0,1). This distribution correctly reproduces the first four moments of the Gaussian distribution. The random numbers were generated using the R250 random number generator in an optimized version for the IBM RS6000 workstations [23].

The most time consuming part of these particle simulations is always the determination of all the pair interactions. To speed this up, a Verlet [24] neighbor list was used in a modification described by Chialvo and Debenedetti [25] which automatically adopts the frequency of update of the neighbor lists to the mobility of the atoms in the simulation. For the system under study, it turned out that the neighbor list had to be updated approximately every 50 fs to correctly keep track of the interacting pairs, meaning that the number of integration steps between neighbor list updates automatically adjusted to 52 for the 1-fs time step, to 12 for the 4-fs time step, and to 5 for the 10-fs time step. The CPU time spent for one time step for the 780 particle system on an IBM RS6000/530H is 0.3 s. An integration based on the algorithm proposed in [4] is about 1.7 times slower. The Nosé-Hoover dynamics in phase space can be implemented equally efficiently but is limited to a maximum time step of about 3 fs.

[1] S. Nosé, J. Chem. Phys. **81**, 511 (1984).
[2] W. G. Hoover, Phys. Rev. A **31**, 1695 (1985).
[3] E. Helfand, Bell Syst. Tech. J. **58**, 2289 (1979); J. Polym. Sci. **73**, 40 (1985).
[4] W. F. van Gunsteren and H. J. C. Berendsen, Mol. Phys. **45**, 637 (1982).
[5] B. Dünweg, J. Chem. Phys. **99**, 6977 (1993).
[6] B. Dünweg and K. Kremer, J. Chem. Phys. **99**, 6983 (1993).
[7] G. Ciccotti and J. P. Ryckaert, Comput. Phys. Rep. **4**, 345 (1986).
[8] H. J. C. Berendsen and W. F. van Gunsteren, in *Molecular Liquids, Dynamics and Interactions,* edited by A. J. Barnes *et al.* (Plenum, New York, 1984), p. 475.
[9] P. A. M. Dirac, Can. J. Math. **2**, 129 (1950); Proc. R. Soc. London, Ser. A **246**, 326 (1958).
[10] W. Rümelin, SIAM J. Numer. Anal. **19**, 604 (1982).
[11] G. N. Milshtein, Theory Probab. Its Appl. **23**, 396 (1978).
[12] A. Greiner, W. Strittmatter, and J. Honerkamp, J. Stat. Phys. **51**, 95 (1988).
[13] G. D. Smith and D. Y. Yoon, J. Chem. Phys. **100**, 649 (1994).
[14] J. L. Anderson and P. G. Bergmann, Phys. Rev. **83**, 1018 (1951).
[15] S. W. de Leeuw, J. W. Perram, and H. G. Petersen, J. Stat. Phys. **61**, 1203 (1990).
[16] V. I. Arnold, V. V. Kozlov, and A. I. Neishtadt, in *Dynamical Systems III,* edited by V. I. Arnold (Springer, New York, 1988), pp. 1–47.
[17] K. Heun, Z. Math. Phys. **45**, 23 (1900).
[18] C. W. Gear, *Numerical Initial Value Problems in Ordinary Differential Equations* (Prentice-Hall, Englewood Cliffs, NJ, 1971).
[19] A. K. Doolittle and R. H. Peterson, J. Am. Chem. Soc. **73**, 2145 (1951).
[20] H. Ertl and F. A. L. Dullien, AIChE J. **19**, 1215 (1973). The reported tridecan values are interpolations based on alkanes of slightly lower and higher molecular weights.
[21] B. Dünweg and W. Paul, Int. J. Mod. Phys. C **2**, 817 (1991).
[22] M. Seeβelberg and F. Petruccione, Comput. Phys. Commun. **74**, 247 (1993).
[23] G. Groten (unpublished).
[24] L. Verlet, Phys. Rev. **159**, 98 (1967).
[25] A. A. Chialvo and P. G. Debenedetti, Comput. Phys. Commun. **60**, 215 (1990).